Scientific Report

On the implementation of the project PN-III-P4-ID-PCE-2016-0122, entitled *Nanostructures for quantum and plasmonic computing* in the period July – December 2017

In the 2017 stage of the project, we focused on the activities

A1.1: Development of a computing algorithm for the investigation of ballistic nanostructures with arbitrary configurations, by extending the computing algorithm developed in the MDEO research center in order to be used for ballistic nanostructures with non-uniform sections and/or bends, and

A1.2: Development of a ballistic configuration for implementing quantum circuits using Y-junction type qubits, by applying the algorithm developed in A1.1 to a Y-junction and finding suitable configurations for implementing logic gates in ballistic nanostructures.

With respect to the last activity, we focused on implementing a quantum algorithm, more precisely on implementing the Fourier transform. The obtained results are detailed in the following.

Development of a computing algorithm for the investigation of ballistic nanostructures with non-uniform sections and/or bends. Application to Y-junctions

The structure analyzed in the 2017 stage of the present project is a graphene nanoribbon, with hydrogen passivated edges, forming a Y-junction with 3 terminals (see Fig. 1). The interest for this structure is motivated by the fact that it can implement position qubits, an incident wavefunction on terminal 1 being divided in two wavefunctions in terminals 2 and 3, such that the outgoing wavefunction can be considered a quantum superposition of the wavefunction in terminals 2 and 3: $a|0\rangle + b|1\rangle$, with $|a|^2 + |b|^2 = 1$, where the quantum logic states $|0\rangle$ and $|1\rangle$ correspond to electronic wavefunctions propagating in terminals 2 and, respectively, 3. Thus, the Y junction generates the input quantum states for many logic gates and algorithms [1,2], the study of ballistic electron transmission through the structure in Fig. 1 being essential for designing logic configurations based on graphene nanoribbons. Although a Y junction could implement quantum logic states in other materials as well, in the ballistic regime, for example in a two-dimensional electron gas (2DEG), we focus on graphene since the mean free path (the average distance between two collisions) is longest in this material [3].

In a symmetric structure, as that in Fig. 1, an electron beam incident from terminal 1 is transmitted with equal probability toward terminals 2 and 3, which implies $T_{12} = T_{13}$, where T_{ij}, i,j = 1,2,3 denotes the transmission coefficient of ballistic electrons incident from terminal i and outgoing via terminal j. As such, the only quantum logic state that can be implemented is $(|0\rangle + |1\rangle)/\sqrt{2}$, which limits the functionality of logic circuits. The aim of the present study is to investigate the possibility of implementing logic states with $a \neq b$ by applying a transversal electric field along the y direction in the beam splitting region (see Fig. 1). Previous experiments and simulations have shown that it is possible in this way to modify the coefficients a and b in the case of a 2DEG satisfying the Schrödinger equation [4,5].

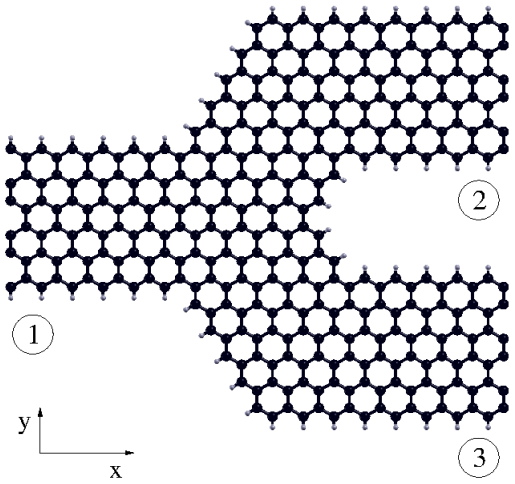

Fig. 1

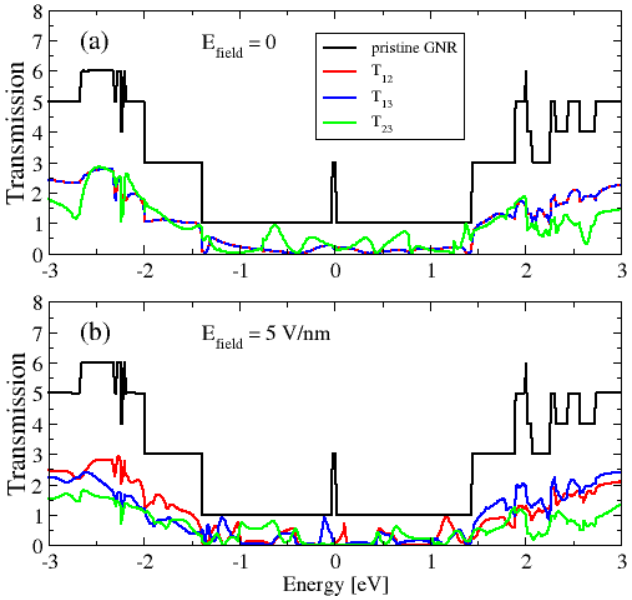

Fig. 2

In this project we have analyzed the ballistic transport in Y junctions from an atomistic perspective, using the density functional theory (DFT). The transmission was calculated using the NEGF (non-equilibrium Green's function) formalism [6] implemented with the TRANSIESTA module of the SIESTA software. In this formalism, the basis functions are strictly localized, which allows the investigation of relatively large systems, of up to several thousand atoms, and is more suited than continuum models to handle very thin nanoribbons, in which the edge effects are important.

To study the transmission through the structure in Fig.1 we consider that terminal 1 is kept at the potential $V_1 = V$, while terminals 2 and 3 are kept at $V_2 = V_3 = 0$. As a first example, we analyzed the total transmission coefficients (as sums on all open channels) in the absence and presence of the electric field E_{field} applied along the y direction, for $V = 0$. The results for T_{12}, T_{13} and T_{23} are represented in Fig. 2(a) and, respectively, Fig. 2(b) as a function of the energy E of incident ballistic electrons, the black line corresponding to the transmission of an ideal straight graphene stripe of the same width. As expected, $T_{12} = T_{13}$ in the absence of E_{field}, terminals 2 and 3 being equivalent in this case (see Fig. 2(a)). On the other hand, by applying E_{field}, with a value of 5 V/nm in Fig. 2(b), T_{12} and T_{13} differ, their values having a maximum on either side of the Fermi level (situated at $E = 0$). From Fig. 2(b) it follows that T_{23} varies also when a transversal electric field is applied, but this transmission coefficient is of no interest in the subsequent studies, only the transmission coefficients T_{12} and T_{13} being relevant for implementing quantum logic states.

To investigate the tenability of the difference between transmission coefficients/currents measured between terminals 1 and 2 and, respectively 1 and 3, we represented in Fig. 3 the two relevant transmission coefficients for different E_{field} values in the 1-10 V/nm range, and for $V = 0$. It can be seen that, for small transversal fields T_{12} and T_{13} are similar, being identical for $E_{field} = 0$, but as the transversal electric field increases T_{12} and T_{13} acquire an anti-phase behavior around the Fermi level: the increase of one transmission at a certain energy E is associated to the decrease of the other one and vice-versa.

By applying a finite voltage between terminals 1 and 2, respectively 1 and 3, for example $V = 0.5$ V, one can estimate the currents I_1 and I_2 measured at terminals 2 and 3 as a function of the applied transversal field. The currents are determined using the Landauer-Büttiker

relation, starting from the transmission coefficients. Fig. 4 illustrates this dependence. The two currents have a non-monotonous behavior, the difference between them vanishing at E_{field} = 6 V/nm, while a moderate field E_{field} = 0.23 V/nm as well as large fields induce a significant difference between the currents at the two terminals. This behavior is due to interferences in the transversal plane of the wavefunctions in all 3 terminals of the device, possible in the ballistic transport regime.

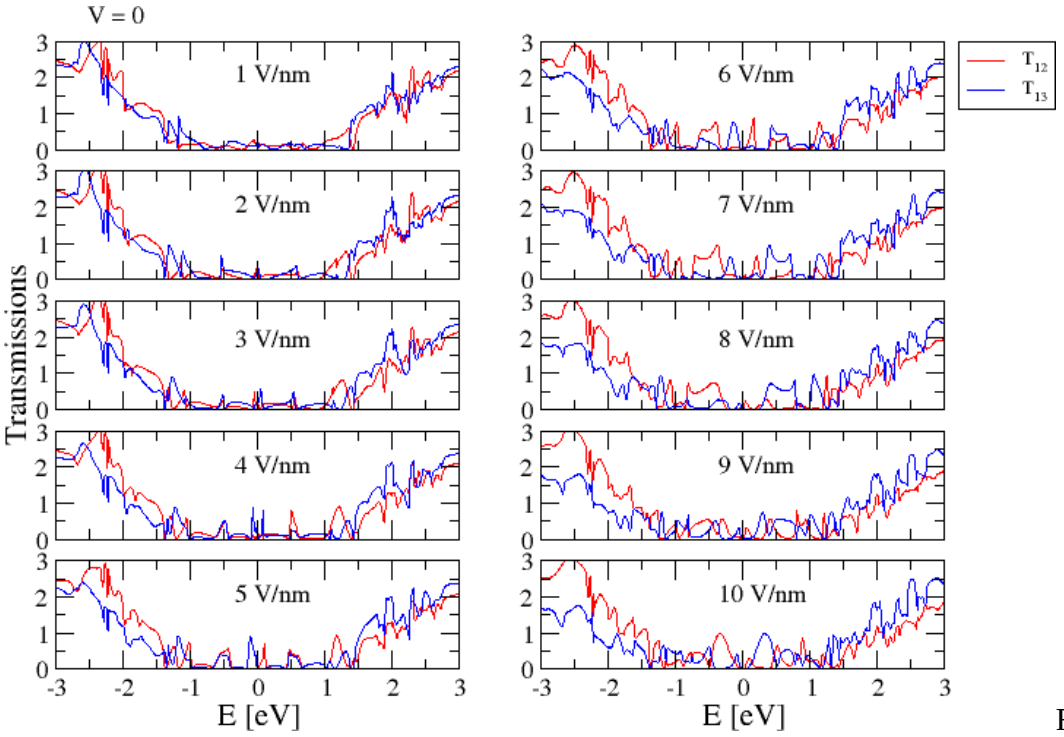

Fig. 3

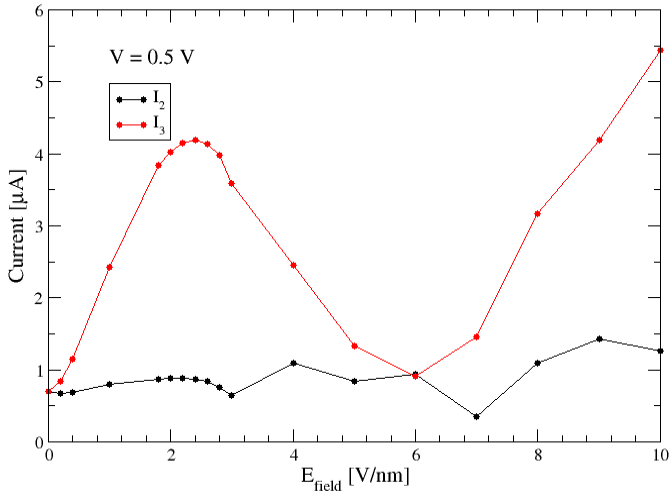

Fig. 4

The bias applied between terminals 1-2 and, respectively 1-3 can influence as well the difference between currents I_1 and I_2, as suggested by Figs. 5(a) and 5(b), corresponding to transversal fields of 5 V/nm and, respectively, 10 V/nm. From these figures it follows that the ratio I_3/I_2 is higher than 1 over the bias interval considered, but depends on E_{field}, being larger for higher transversal fields, in agreement with Fig. 4. The unexpected result is that, even in this case, the ratio I_3/I_2 depends non-uniformly of the bias, reaching a maximum value for V = 0.6 V when E_{field} = 10 V/nm. This behavior is caused by the potential modulation along x via the applied bias, modulation that influences the interference of wavefunctions in all terminals.

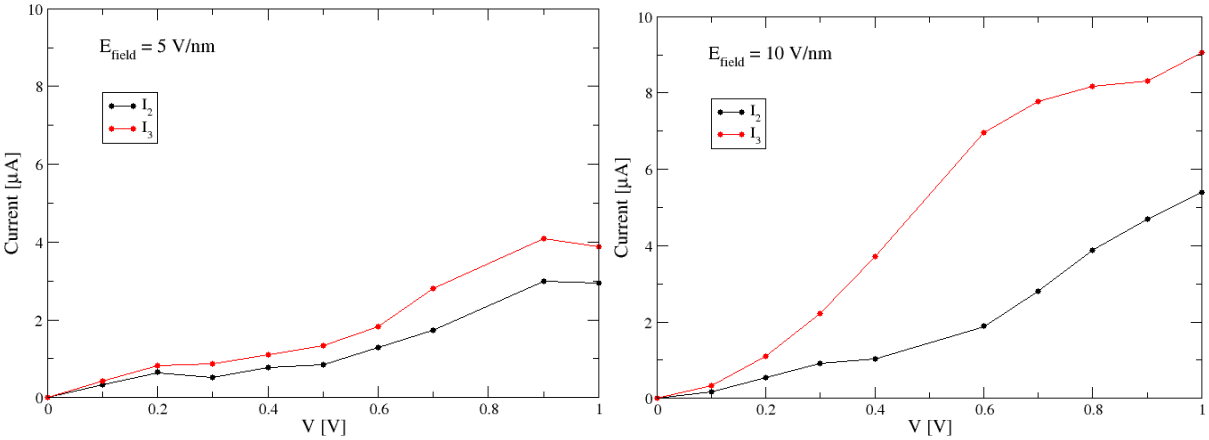

Fig. 5 (a) (b)

In conclusion, a transversal electric field can commute the current between the two arms/branches of a Y junction; the arm with a larger current is determined by the direction of the transversal electric field, the respective currents in terminals 2 and 3 switching their values as the direction of the field is reversed. The ratio between the two currents is not monotonous as a function of the transversal electric field or as a function of the applied voltage, optimum values existing for maximizing this effect.

Another possibility of inducing a difference between the transmission coefficients/currents in the outgoing terminals of a Y junction is to use asymmetric configurations, as those illustrated in figures 6(a) and 6(b), referred to in the following as thin branch and thick branch configurations, respectively.

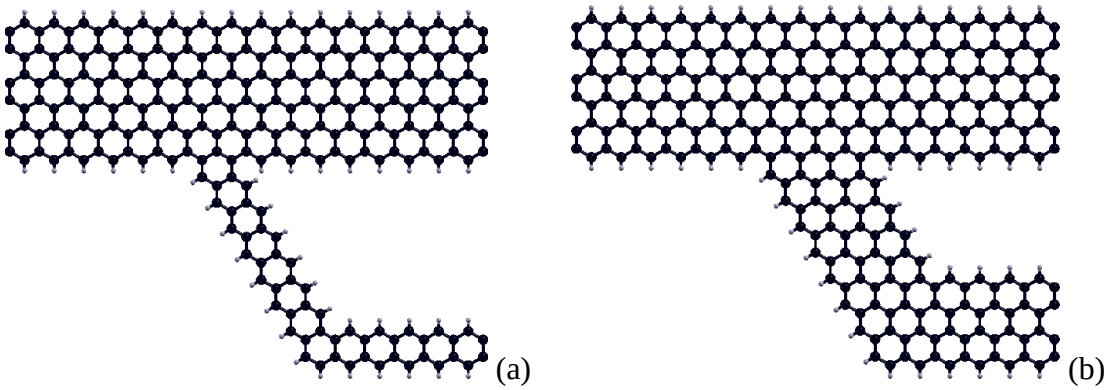

Fig. 6 (a) (b)

The dependence of the corresponding transmission coefficients on the energy of ballistic electrons is represented in Fig. 7. From this figure it can be seen that in junctions with a narrow branch T_{12} is close to the ideal transmission, while T_{13} is significantly reduced. The presence of minima in T_{12} is caused by the resonant transport/wavefunction interferences in the 3 terminals of the junction. These minima become wider as the coupling of the lateral branch increases (the thick branch case), behavior associated with a decrease of T_{12}.

It should be mentioned that, for some energies of the incoming electrons, T_{12} or T_{13} vanish in symmetric junctions subjected to transversal electric fields (see Fig. 3) as well as in asymmetric junctions (see Fig. 7), which is a requirement for optimum behavior of NOT and CNOT quantum logic gates [1]. The condition $T_{12} = 0$ or $T_{13} = 0$ for a given energy E of the incident electrons, tunable via a gate voltage, can be achieved in the first case by varying E_{field}, which assumes the fabrication of additional electrodes in the junction plane, while in the second case it implies a proper choice of geometry.

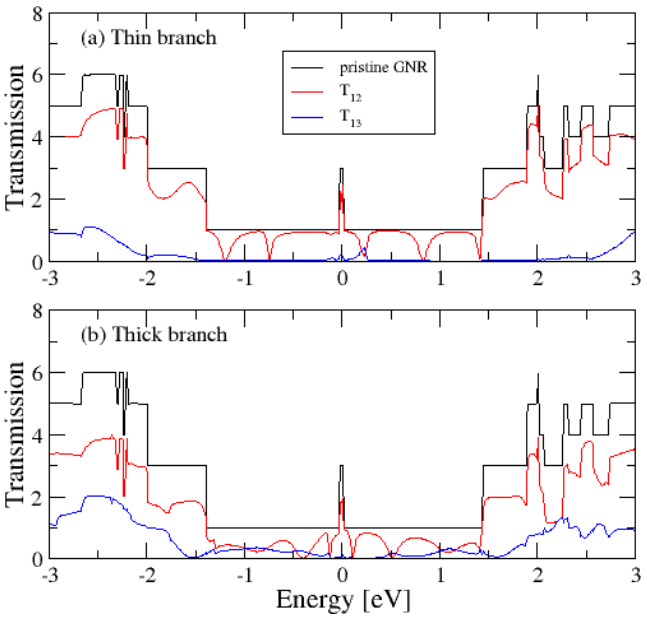

Fig. 7

The original results obtained by atomistic simulation of ballistic charge transport in graphene through Y junctions are going to be finalized and submitted for publication (**A1**).

Development of configurations for the implementation of the discrete quantum Fourier transform in ballistic nanostructures

In a previous paper [1] graphene configurations were shown to be able to implement several logic gates, since this material has the longest mean free path, and thus allows the fabrication of logic gates/circuits working in the ballistic (coherent/collisionless) regime. Logic circuits of practical interest, however, implement algorithms, which are generally realized as succession of logic gates. Such an approach assumes that the mean free path is longer than the circuit's dimension, requirement that limits the number of logic gates that can be successively implemented.

In the project we have focused on implementing an algorithm, more specific the quantum discrete Fourier transform (DFT), which is a component of other algorithms, such as the Shor algorithm. The quantum DFT applied to an *n*-qubit state is defined as

$$F:\sum_{j=0}^{N-1} x_j \,|\, j\rangle_n \rightarrow \sum_{k=0}^{N-1} y_k \,|\, k\rangle_n \qquad (1)$$

and can be obtained by a succession of Hadamard logic gates H, conditional rotation gates represented by matrices

$$R_k = \begin{pmatrix} 1 & 0 \\ 0 & \exp(2\pi i / 2^k) \end{pmatrix} \qquad (2)$$

and SWAP gates represented by 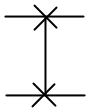 in the circuit in Fig. 8 [7].

Quantum circuits of Hadamard and conditional rotation types can be implemented with graphene nanoribbons based on Y junctions, by a proper choice of the lengths of interference regions L_H and L_R. The working principle of these gates is discussed in details in [1], and the Y junction simulations presented above are essential for finding the optimum working conditions of these gates.

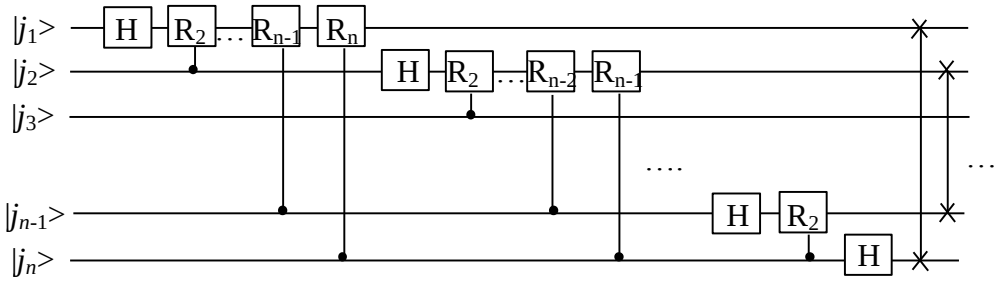

Fig. 8

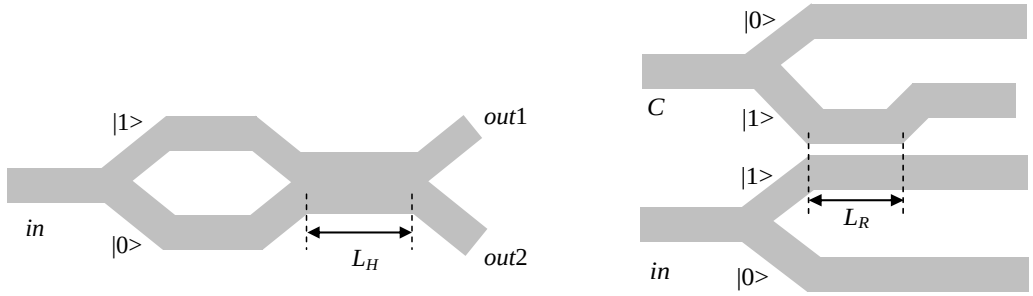

Fig. 9 (a) (b)

A circuit that realizes the quantum DFT involves thus coupling Hadamard and conditional rotation gates, as in Fig. 8, the SWAP gates being dispensable if the output qubits are properly defined. The resulting circuit is both complex and long, even for a small number of input qubits, imposing constrains on the material and working temperature. Such a solution for DFT implementation is not feasible. Therefore, we look for a direct implementation of the DFT of a quantum electronic wavefunction, without decomposing it in logic gates. More precisely, we propose a configuration that realizes the continuous Fourier transform of the wavefunction, configuration that can be then discretized to implement the DFT in nanostructures.

The Fourier transform of a function $\psi(x)$ is a particular case, for $\alpha = \pi/2$, of the fractional Fourier transform (FFT) of order α, defined as [8]

$$F_\alpha \psi(x') = \sqrt{\frac{\exp[i(\pi/2-\alpha)]}{2\pi \sin\alpha}} \int \psi(x) \exp\left(-i \frac{x^2 + x'^2}{2\tan\alpha} + i \frac{xx'}{\sin\alpha} \right) dx . \qquad (3)$$

The FFT implementation method for ballistic electrons put forward in this project relies on the analogy between the classical electromagnetic field and the wavefunction of ballistic electrons [9] and on the fact that the FFT in optics is achieved in a graded-index (GRIN) waveguide, with a refractive index $n(x)$ that varies quadratically in the transverse direction [8,10]. As such, a FFT of tunable order can be realized in 2DEG or graphene subjected to a gate voltage that induces a potential energy quadratically dependent on x: $U_G(x) = U_0 + \gamma x^2$, where the second term can be considered a perturbation of the first one. In a 2DEG, the wavefunction $\Psi(x, y) = \psi(x)\exp(iky)$ of electrons with effective mass m that propagate with a wavenumber k along direction y is a solution of the time-independent Schrödinger equation:

$$\left[-\frac{\hbar^2}{2m}\left(\frac{\partial^2}{\partial x^2}+\frac{\partial^2}{\partial y^2}\right)+U_G(x)-E\right]\Psi=0 \tag{4}$$

The equation above is similar to the Helmholtz equation

$$\left(\frac{\partial^2}{\partial x^2}+\frac{\partial^2}{\partial y^2}+k_0^2 n^2(x)\right)E(x,y)=0,\quad k_0=\omega/c \tag{5}$$

satisfied by the electric field of an electromagnetic wave $E(x,y)=E(x)\exp(iky)$ with frequency ω, which propagates along y in a GRIN medium with $n(x)=n_0-n_1x^2/2$, where the second term is much smaller than the first. Since the GRIN medium realizes a FFT of order α of the incident field after a propagation distance $L_\alpha=\alpha\sqrt{n_1/n_0}$ [8,10], the potential induced by the gate electrode implements a FFT of order α after a propagation distance in 2DEG equal with

$$L_\alpha=\alpha\sqrt{(E-U_0)/\gamma} \tag{6}$$

In both cases, the trajectory of ballistic electrons/electromagnetic field is periodic, the position x and the tangent to the trajectory θ in a plane y = const. evolving with respect to the corresponding parameters in the plane y = 0 (indexed by 0) as:

$$\begin{pmatrix}x\\ \theta\end{pmatrix}=\begin{pmatrix}\cos(Ay) & \dfrac{\sin(Ay)}{A}\\ -A\sin(Ay) & \cos(Ay)\end{pmatrix}\begin{pmatrix}x_0\\ \theta_0\end{pmatrix} \tag{7}$$

with $A=\sqrt{n_1/n_0}$ in optics and $A=\sqrt{(E-U_0)/\gamma}$ for electrons in a 2DEG.

If the quadratic potential is applied to a graphene stripe, in which the spinorial wavefunction $\Psi^T=(\psi_1,\psi_2)$ that propagates along y with a wavenumber k satisfies the equation

$$\hbar v_F\begin{pmatrix}0 & -i\dfrac{\partial}{\partial x}-ik\\ -i\dfrac{\partial}{\partial x}+ik & 0\end{pmatrix}\begin{pmatrix}\psi_1\\ \psi_2\end{pmatrix}=(E-U_G)\begin{pmatrix}\psi_1\\ \psi_2\end{pmatrix} \tag{8}$$

where $v_F\cong c/300$ is the Fermi velocity, it can be shown that each spinor component is a solution of

$$\left[\hbar^2 v_F^2\left(-\frac{\partial^2}{\partial x^2}+k^2\right)-[E-U_G(x)]^2\right]\psi_{1,2}=0, \tag{9}$$

the FFT of order α being obtained after a propagation distance

$$L_\alpha=\alpha\sqrt{(E-U_0)/2\gamma} \tag{10}$$

This distance is $\sqrt{2}$ times shorter than that required to obtain a similar effect in 2DEG, being a manifestation of the Berry phase in this [11]. The trajectory of charge carriers is periodic in this case also, described by equation (7) with $A = \sqrt{(E - U_0)/2\gamma}$

A parabolic potential distribution can be realized with a nonplanar, convex or concave, gate electrode, as in Fig. 10. Areas of convex or concave electrodes have been fabricated on flexible substrates [12], while individual nonplanar electrodes with complex topographies at nanometer scale were fabricated with lithographic techniques [13].

Because $\gamma > 0$, the configuration in Fig. 10(a) realizes a FFT for negative potentials U_G, while that in Fig. 10(b) achieves this for positive U_G, the latter configuration needing a shorter length L for implementing a FFT with a given α.

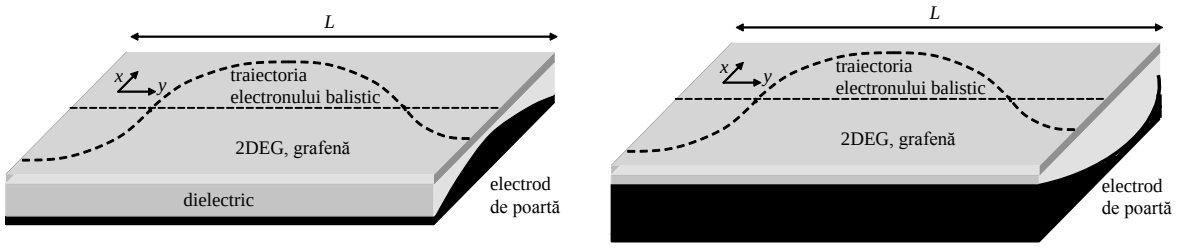

Fig. 10 (a) (b)

Another, simpler technological solution is to fabricate a segmented gate electrode, consisting of several metallic stripes of equal or different widths, as shown in Fig. 11(a) and, respectively, 11(b); the distance between electrodes, d, is considered constant.

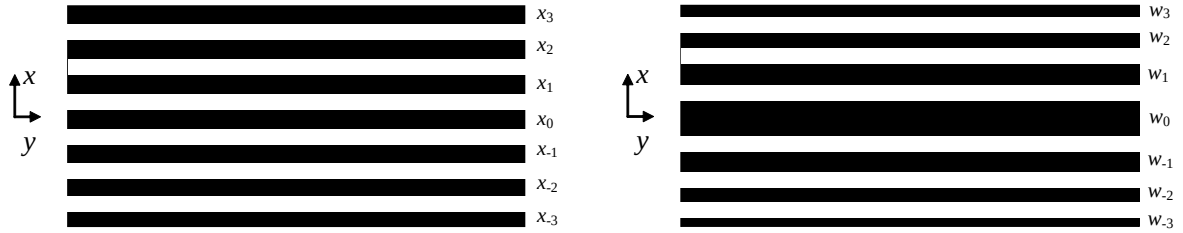

Fig. 11 (a) (b)

In the first case the metallic electrodes of equal widths must be connected independently, the gate potential applied on electrode n, with a center coordinate x_n being chosen to induce a potential $U_n = U_G(x_n)$ if d is small, or

$$U_n(x_n + d) = \int_{x_n - d}^{x_n + d} (U_0 + \gamma x^2)dx \qquad (11)$$

if d cannot be neglected. In the second case, a parabolic potential can be implemented by a segmented electrode in which all segments are connected to the same gate voltage that induces a potential U if the width of electrode n, w_n, is chosen such that

$$U(x_n + d) = \int_{x_n - d}^{x_n + d} (U_0 + \gamma x^2)dx \qquad (12)$$

where x_n is the center of electrode n and satisfies the relation $x_{n+1} = x_n + d + (w_n + w_{n+1})/2$. Equations (11) and (12) express the fact that the average potential is the same in a segmented and a continuous electrode [14].

The parabolic potential $U_G(x) = U_0 + \gamma x^2$ can thus generate a FFT of order α after a propagation length L_α for the wavefunction of ballistic electrons in 2DEG or graphene. In particular, the continuous Fourier transform is obtained after a propagation distance $L_{\pi/2}$ and the DFT can be generated by discretizing both input and output wavefunctions, as suggested in Fig. 12.

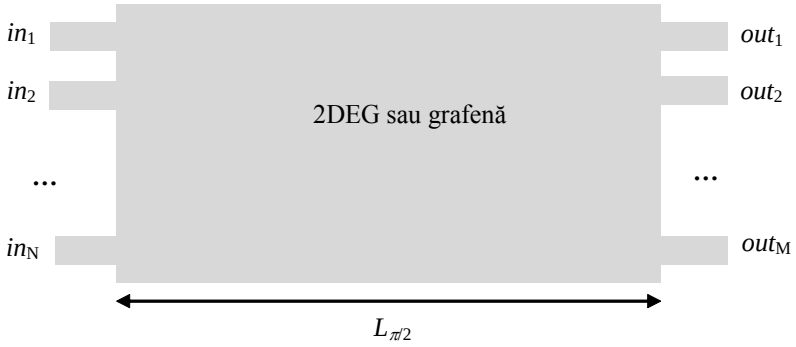

Fig. 12

The original results regarding the implementation of FFT of order α of an electronic wavefunction in 2DEG or graphene are submitted for publication (**A2**).

References

[1] D. Dragoman, M. Dragoman, J. Appl. Phys. **119**, 094902 (2016).

[2] D. Dragoman, M. Dragoman, Nanotechnology **26**, 485201 (2015).

[3] A.S. Mayorov, R.V. Gorbachev, S.V. Morozov, L. Britnell, R. Jail, L.A. Ponomarenko, K.S. Novoselov, K. Watanabe, T. Taniguchi, A.K. Geim, Nano Lett. **11**, 2396 (2011).

[4] T. Palm, L. Thylén, Appl. Phys. Lett. **60**, 237 (1992)

[5] G.M. Jones, C.H. Yang, M.J. Yang, Y.B. Lyanda-Geller, Appl. Phys. Lett. **86**, 073117 (2005).

[6] G.A. Nemneş, C. Vişan, A. Manolescu, J. Mater. Chem. C **5**, 4435 (2017).

[7] F.L. Marquezino, R. Portugal, F.D. Sasse, J. Comput. Appl. Math. **235**, 74 (2010).

[8] H.-Y. Fan, Y. Fan, Commun. Theor. Phys. **39**, 97 (2003).

[9] D. Dragoman, M. Dragoman, Prog. Quantum Electron. **23**, 131 (1999).

[10] D. Mendlovic, H.M. Ozaktas, A.W. Lohmann, Appl. Opt. **33**, 6188 (1994).

[11] K.S. Novoselov, E. McCann, S.V. Morozov, V.I. Fal'ko, M.I. Katsnelson, U. Zeitler, D. Jiang, F. Schedin, A.K. Geim, Nature Phys. **2**, 177 (2006).

[12] Z. Xiang, J. Liu, C. Lee, Microsyst. Nanoeng. **2**, 16012 (2016).

[13] F. Yesilkoy, V. Flauraud, M. Rüegg, B.J. Kim, J. Brugger, Nanoscale **8**, 4946 (2016).

[14] V.V. Kotlyar, A.A. Kovalev, A.G. Nalimov, J. Opt. **15**, 125706 (2013).

Papers to be finalized/submitted for publication in ISI journals in 2017

A1: G. Nemneş, T.L. Mitran, D. Dragoman – Ab initio investigations of ballistic graphene Y-junctions in transversal electric field, to be finalized and submitted at J. Appl. Phys.

A2: D. Dragoman – Tunable fractional Fourier transform implementation of electronic wavefunctions in atomically thin materials, submitted at Nanotechnology

Project Director,

Prof.univ.dr. Daniela Dragoman